Optical Engineering

OpticalEngineering.SPIEDigitalLibrary.org

Cryogenic application of an autocentering mount working at the diffraction limit

Beatriz Sánchez
Carolina Keiman
Jorge Fuentes-Fernández
Salvador Cuevas
Carlos Espejo
Oscar Chapa
Rubén Flores-Meza
Luis Carlos Álvarez
Gerardo Lara
Leonardo Garcés

SPIE.

Beatriz Sánchez, Carolina Keiman, Jorge Fuentes-Fernández, Salvador Cuevas, Carlos Espejo, Oscar Chapa, Rubén Flores-Meza, Luis Carlos Álvarez, Gerardo Lara, Leonardo Garcés, "Cryogenic application of an autocentering mount working at the diffraction limit," *Opt. Eng.* **56**(3), 034114 (2017), doi: 10.1117/1.OE.56.3.034114.

Cryogenic application of an autocentering mount working at the diffraction limit

Beatriz Sánchez,* Carolina Keiman, Jorge Fuentes-Fernández, Salvador Cuevas, Carlos Espejo, Oscar Chapa, Rubén Flores-Meza, Luis Carlos Álvarez, Gerardo Lara, and Leonardo Garcés
Universidad Nacional Autónoma de México, Instituto de Astronomía, Ciudad Universitaria, Mexico City, Mexico

Abstract. We present the design concept and validation of a cryogenic lens mount for a noncemented doublet for the near-infrared diffraction limited instrument FRIDA. The design uses an autocentering mount that maintains the relative alignment of the lenses, acting against any displacement that may be induced by external forces by automatically returning the lenses to their nominal positions. Autocentering techniques have been used for instruments at room temperature with relatively relaxed image quality requirements. We present in detail its application to a mount for a cryogenic instrument working at the diffraction limit. The design has been tested on the collimator of FRIDA, a noncemented doublet of CaF_2 and S-FTM16. We describe the alignment requirements of the system, and we show the calculations that ensure that the lenses will suffer both appropriate stresses and temperature differences. We present the experimental validation of a prototype, demonstrating that the design delivers an excellent performance without inducing unnecessary stresses on the optical components, provided that the lenses are previously aligned with very high precision. [DOI: 10.1117/1.OE.56.3.034114]

Keywords: optomechanical design; astronomy; infrared.

Paper 170119 received Jan. 23, 2017; accepted for publication Mar. 7, 2017; published online Mar. 24, 2017.

1 Introduction

Optomechanical supports have been a widely discussed subject in the field of instrumentation by authors such as Yoder,[1] Fischer et al.,[2] and Ahmad,[3] to name a few. Nonetheless, lens mounts in infrared cryogenic instruments, in particular when they have to work at the diffraction limit of the telescope, still represent a big challenge due to the thermal compressions to which the optomechanical system has to be exposed and the high image quality requirements. In addition, these systems often involve combinations of different materials with varying coefficients of thermal expansion (CTE). Lens systems, for example, can be combinations of materials such as calcium fluoride, fused silica, or S-FTM16, generally mounted in aluminum or stainless steel barrels.[4]

An effective design for such a system must consider the different CTEs in play, the thermal stresses that are induced by changes in temperature (typically, from 295 to 150 K or even colder), the geometry of the different parts, the number of components, etc. In spite of a lot of experience in the development and fabrication of these components, successful results are not guaranteed by a standard solution since the recipes that exist for mounts at room temperature are not directly applicable in cryogenic conditions, so specific considerations need to be taken into account.

Ensuring the desired performance of a cryogenic instrument presents a big challenge. In particular, the alignment of the optical components must be optimal at the operational temperatures, but lenses can only be aligned at room temperatures in the assembly laboratory. The instrument then needs to be transported from the assembly laboratory to the telescope's site, and, once there, it will typically perform several cool-downs and warm-ups per year. In general terms, optomechanical mounts for near-infrared instruments working at cryogenic temperatures must satisfy the following requirements:

1. Lenses have to be aligned at the lab and at room temperature.
2. The force supporting the lenses has to be enough to avoid misalignments during transportation.
3. Lenses have to maintain their alignment when cooled down to the operational temperature.
4. The optomechanical mounts must guard against excessive thermal shocks on the lenses.
5. Once the operational temperature has been reached, the optomechanical mounts must avoid excessive temperature gradients on the lenses, which may lead to local variations of the refractive index and produce excessive wavefront errors.

For cryogenic instruments of this kind, the optomechanical mounts tend to be quite complex since they typically use a support system that restricts the movement of the lenses to tilts and along the lens radial direction (where the thermal compression is relatively larger). These are usually combined with a normal support (normal to the lens' surface) that holds the lenses to their position.[5–10] Such designs require very high precision centering of the lens edge with respect to its optical axis, and this centering precision must be better than the positional tolerances of the lens, usually several micrometers. Moreover, it impedes the natural movement

*Address all correspondence to: Beatriz Sánchez, E-mail: beatriz@astro.unam.mx

of the lenses on each mechanical support, which in most cases is not a radial movement but is rotational around the center of curvature of the surface in contact with the mechanical support. This induces unnecessary stresses that may fracture the lenses.[10]

A simpler and less restrictive mounting alternative uses the principle of autocentering described by Yoder[1] and Zschommler.[11] This principle guarantees, under certain conditions, the autocentering of the lenses on the mount's mechanical axis using only a normal support and allowing for rotational movement. Autocentering can be achieved with a lens-mount contact of sphere-cone type (tangential contact) or sphere-torus type (toroidal contact). We note that, in principle, this is only valid for spherical surfaces.

Autocentering techniques have been used for instruments at room temperature with relatively relaxed image quality requirements. However, to our knowledge, they have never been reported for cryogenic instruments, especially when they have to work at the diffraction limit of a large telescope in the near-infrared regime. This is partly because, as we shall see, an autocentering mount on its own does not produce the fine relative alignment required by such instruments. The key aspect in this paper is that, as we will demonstrate in Sec. 3.1, while autocentering on its own is not enough, by prealigning the lenses to the required precision, the autocentering mount maintains this alignment with very high precision under the typical conditions that a cryogenic instrument may suffer over its entire life.

The optomechanical design presented in this article arose to satisfy the need for a simpler mount than those commonly in use for the refractive optical components of FRIDA (infrared imager dissector for adaptive optics).[12–14] The instrument's optomechanical design is based on noncemented achromatic doublets of calcium fluoride (CaF_2) and Ohara S-FTM16[15] or Infrasil® 301. FRIDA will be the first instrument for the Gran Telescopio de Canarias (GTC) designed to achieve the diffraction limit of the telescope using the GTC adaptive optics system. The design uses the principle of autocentering, supporting one side of the lens with a fixed mechanical support and the other side with cantilever springs to maintain the lens toward the fixed support and compensate for the different CTEs of the lenses and their mounts. In contrast with Yoder[1] and Zschommler,[11] the lenses are previously aligned in the laboratory with a precision of ± 14 μm between the vertices of the two lenses in the radial direction. The role of the autocentering mount is not then to center the lenses in their positions, but to maintain their alignment when they are exposed to external forces such as those that they will suffer during transportation, cool-downs, and warm-ups. The design was tested on the optomechanical mount for the collimator of FRIDA, a noncemented achromatic doublet formed by one concave/convex S-FTM16 divergent lens and one biconvex CaF_2 convergent lens.

The article is structured as follows. Section 2 presents the requirements that the optomechanical mounts of FRIDA must satisfy. In this section, we pay special attention to the alignment requirements to ensure a high Strehl ratio and show the calculations to determine the maximum stresses on the lenses based on experimental work, the maximum temperature differences during cool-downs and warm-ups to avoid fractures, and the maximum temperature differences during operation to preserve a high quality transmitted wavefront. Section 3 presents the design concept with emphasis on the principles on which the design is based, including a calculation of the forces needed to be applied by the normal support. Sections 4–6 present the methodology used to experimentally validate the optomechanical mount and the results of the tests performed, demonstrating that the lenses fulfill all the requirements. Finally, Sec. 7 presents a summary of the work done and some conclusions.

2 Optomechanical Requirements

2.1 *Maximum Misalignment*

As FRIDA is designed to operate at the diffraction limit of a large telescope, its optics shall maintain an excellent image quality after the processes of transportation and cooling down to cryogenic temperatures. Optical tolerancing studies give a strong limit on the relative alignment of the lenses within each doublet. The high level requirements for image quality of the instrument demand a Strehl ratio better than 0.7, which, at the subsystem level, requires a Strehl ratio better than 0.95 for each doublet. The Zemax tolerancing analysis was done by simulating the rotational movements of the lenses around the center of curvature of the surfaces in contact with the fixed mechanical support. From those tolerances, we deduced the maximum allowed misalignment between the two lenses, in the radial direction, to be 115 μm.

2.2 *Minimum Restraining Force*

The lenses of FRIDA will be mounted and aligned at the IA-UNAM (Instituto de Astronomía, Universidad Nacional Autónoma de México) and will have to be transported to the telescope's site on the island of La Palma, in the Canary Islands. According to the "handling and storage" requirement from the GTC, the maximum allowed shock acceleration of the instrument during transportation shall be 10 g. Therefore, the optomechanical mount shall exert a frictional force equivalent to at least 10 g to preserve the alignment within the specified tolerances during transportation.

2.3 *Maximum Mechanical Stress*

While a minimum stress is necessary to maintain alignment during transportation, as described above, the optomechanical mount shall not exert stresses large enough to cause them to fracture. Due to thermal expansion, the lenses will suffer the maximum stresses during cool-downs. To calculate the fracture probability, we assume that during the 20-year life of FRIDA, the lenses will be cooled down at least 50 times. FRIDA contains nearly 20 lenses, so we require no fractures in a total of 1000 events. Accepting the probability of fracture of one event to be 0.01, then the fracture probability of each lens shall be less than 10^{-5}.

The maximum stress on the CaF_2 lens is calculated from the results of Klein,[16] using Weibull's statistical theory of fracture with a bimodal distribution by which the defects are distributed in two distinct modes. The bimodal fracture probability, P, as a function of the applied stress, σ, is then given by

$$P(\sigma)=1-W\exp\left\{-\pi\left(\frac{r_0}{\mathrm{cm}}\right)^2\left[\Gamma\left(1+\frac{1}{m_1}\right)\right]^{m_1}\left(\frac{\sigma}{\sigma_{C1}^{bi}}\right)^{m_1}\right\}$$
$$-(1-W)\exp\left\{-\pi\left(\frac{r_0}{\mathrm{cm}}\right)^2\left[\Gamma\left(1+\frac{1}{m_2}\right)\right]^{m_2}\left(\frac{\sigma}{\sigma_{C2}^{bi}}\right)^{m_2}\right\}, \quad (1)$$

where W and $(1-W)$ are the fractions belonging to the first and second modes (subindices 1 and 2), r_0 (in centimeters) is the diameter of the loading ring where the lens makes contact with the support mechanical part, and Γ is the gamma factorial function. Each of the two modes is characterized by two parameters, σ_C^{bi} and m, the characteristic strength and the Weibull modulus, respectively. The experimental values obtained for CaF_2 are taken from Klein,[16] as $\sigma_{C1}^{bi}=60.6$ MPa, $m_1=6.9$, $\sigma_{C2}^{bi}=104$ MPa, and $m_2=6.11$, for a fraction coefficient of $W=0.464$. Combining this value with the parameters from Eq. (1), we get that the maximum stress on the CaF_2 lens shall be $\sigma=7.3$ MPa.

The maximum stress on the S-FTM16 lens is estimated from the Schott technical note TIE-33,[17] which shows the coefficients for a monomodal Weibull statistic to calculate the fracture probability of glasses BK7, F2, and Zerodur®. The Ohara glass S-FTM16 is very similar to the Schott glass F2 both in its optical and mechanical parameters. Therefore, we considered the Weibull coefficients of F2 for S-FTM16. Analogously to Eq. (1), the monomodal fracture probability is given by

$$P(\sigma)=1-\exp\left\{-\pi\left(\frac{r_0}{\mathrm{cm}}\right)^2\times\left[\Gamma\left(1+\frac{1}{m}\right)\right]^{m}\left(\frac{\sigma}{\sigma_0}\right)^{m}\right\}, \quad (2)$$

where, for F2, we have $\sigma_0=57.1$ MPa and $m=25$. For a fracture probability less than 10^{-5}, the maximum stress on the S-FTM16 lens shall finally be $\sigma=31$ MPa.

2.4 *Maximum Thermal Stress*

The optomechanical mount shall avoid thermal differences during cool-downs and warm-ups that will induce stresses larger than those from Sec. 2.3. The thermal stress induced by a temperature difference in the lens, ΔT, is given in the Schott technical note TIE-32,[18] as

$$\sigma=f\frac{\alpha E}{1-\mu}\Delta T, \quad (3)$$

where f is a correction factor, α is the CTE, E is the Young's modulus, and μ is the Poisson's ratio. The correction factor f takes the value of 1 if we are dealing with an instantaneous thermal shock (i.e., with no time for the thermal conduction mechanisms to begin stabilizing the glass); it takes the value of 0.5 to 0.7 for moderate temperature changes in which thermal conduction could be compensating the thermal stress and can be less than 0.5 for very slow temperature changes. The rest of the terms are commonly gathered in the so-called thermal stress factor, defined as

$$\phi=\frac{\alpha E}{1-\mu}. \quad (4)$$

Given the specific parameters of the materials, we get $\phi=1.88$ MPa/K for CaF_2 and $\phi=0.76$ MPa/K for S-FTM16. From Eqs. (3) and (4), we then get

$$\Delta T=\frac{\sigma}{f\phi}, \quad (5)$$

And, with the maximum stress values from Sec. 2.3, taking the correction factor of 0.7, we get the maximum temperature differences that the lenses can hold without fracturing during cool-downs and warm-ups as $\Delta T<5.5$ K for CaF_2 and $\Delta T<58.3$ K for S-FTM16.

2.5 *Maximum Temperature Differences during Operation*

Temperature differences during operation may induce changes in the optical path due to changes in the refractive index, n, and thickness, w, of the lenses. These changes in the optical path are given by

$$\delta=w(n-1)\alpha\Delta T+w\frac{\mathrm{d}n}{\mathrm{d}T}\Delta T, \quad (6)$$

and

$$\Delta T=\frac{\delta}{w\left[(n-1)\alpha+\frac{\mathrm{d}n}{\mathrm{d}T}\right]}. \quad (7)$$

The tolerance in surface figure of the lenses, as determined by the tolerancing analysis, shall be 0.5λ (He–Ne laser wavelength) or 0.25 fringes for each lens in order for the total Strehl ratio of the instrument not to degrade beyond the specifications. We assume that the wavefront error (WFE) induced by thermal gradients of the refractive index must be about four times smaller than those induced by the surface figure of the lenses. Hence, the maximum values of the WFE induced by thermal effects shall be less than $\delta=80$ nm. Using Eq. (7), we get that, for the two lenses of the collimator of FRIDA, the maximum temperature differences shall be 1.27 K for the CaF_2 lens and 5.96 K for the S-FTM16 lens.

3 Design Concept

3.1 *Spring Supports*

A diagram of the lenses of the collimator of FRIDA inside the optomechanical cell is shown in Fig. 1. The lenses rest on a fixed support, held by a spring support that maintains the lenses toward the fixed support applying forces only in the normal direction to their surfaces. This allows the lenses to move on their mechanical mounts around the center of curvature of the surface in contact with the fixed support. According to the nature of the lens, it will have a sphere-cone type contact for the convex surfaces (tangential contact) and a sphere-torus type contact for the concave surfaces (toroidal contact). Because lenses are typically much thinner than their diameter, they will typically suffer a lower change in dimensions in between the mechanical support than using a radial support.

The autocentering potential of each lens is defined as the linear misalignment that would result when the lens is autocentered, if it has not been previously aligned. This is empirically given by the wedge angle, θ, formed at the intersection of the two tangent lines to the two lens surfaces at

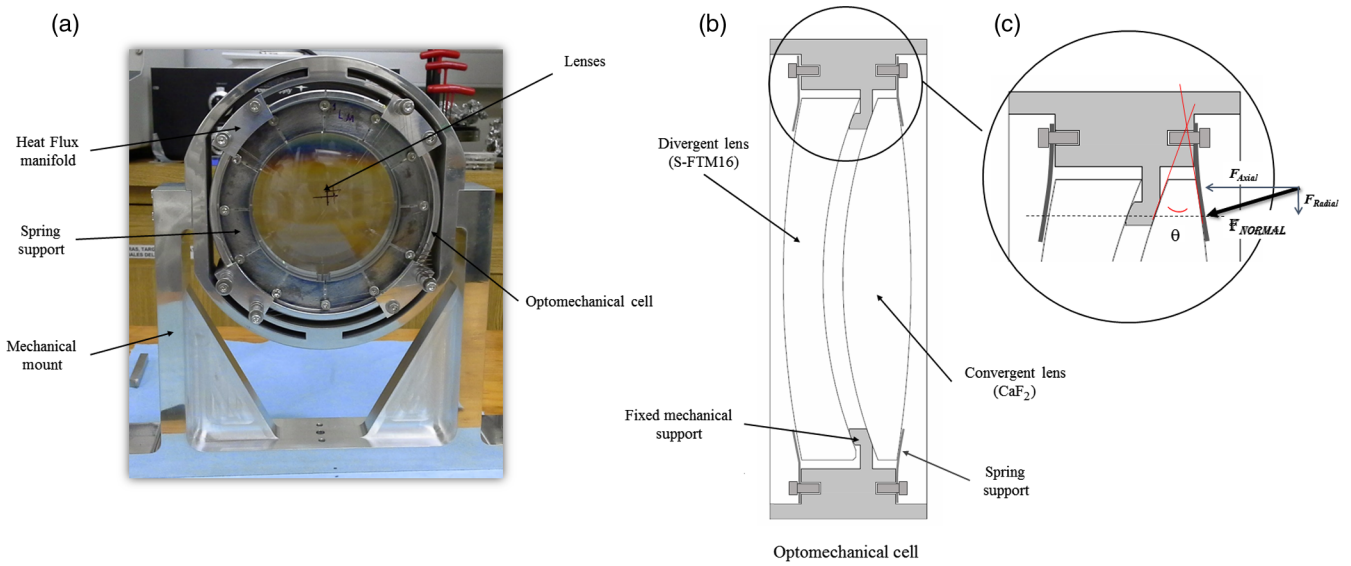

Fig. 1 (a) Picture and (b) diagram of the lenses of the collimator of FRIDA inside the optomechanical cell. In (c), we show the wedge angle, θ, for the convergent lens, and the normal force applied by the spring, which may be decomposed in an axial and a radial component.

the points of contact with the optomechanical support, as shown in Fig. 1(c).[11] The wedge angle takes the value of 27.2 deg and 10 deg for the convergent (CaF_2) and divergent (S-FTM16) lenses of the collimator of FRIDA, respectively. Following the empirical relation given by Zschommler,[11] the respective autocentering potentials are 30 and 130 μm, which correspond to a rotation of the two lenses of 0.8 and 3 arcmin, respectively, around the corresponding centers of curvature. In the worst case, these two sum to a maximum relative misalignment of 160 μm. This is worse than the results obtained from the tolerancing analysis discussed in Sec. 2.1, which gives a maximum relative misalignment of 115 μm. In practice, as will be shown in the following sections, we have the capability of aligning the lenses a priori to within 14 μm; hence, we expect a much better performance. The experiments carried out in this article demonstrate that the autocentering mount maintains the relative alignment of the lenses well below the maximum allowed values given by the Zemax tolerancing analysis.

The spring support will use cantilever springs. It is designed to give the necessary forces on the lenses without applying unnecessary stresses, despite the differences in the CTE's in play. The spring support is composed of a ring of 12 cantilever plates that rest directly on the lens surface [see Fig. 1(b)]. According to Hooke's law, the force exerted by the springs is directly proportional to the spring displacement, ϵ, and the spring constant, k, given by the moment of inertia of each plate and its Young's modulus, following the expression

$$F_{\text{normal}} = \frac{Ebh^3}{l^3}\epsilon = -k\epsilon, \tag{8}$$

where E is the Young's modulus and b, h, and l are the spring's width, thickness, and length, respectively. As shown in Fig. 1(c), this force can be decomposed into a radial component (perpendicular to the optical axis) and an axial component (parallel to the optical axis). We expect that during transportation, the lenses will suffer accelerations, mostly in the radial directions, no larger than 10 g. According to the model proposed by Yoder,[1] the radial force that each spring plate has to exert is given by

$$F_{\text{radial}} = \frac{Wa_{\text{radial}}}{\mu}\cos\theta, \tag{9}$$

where W is the lens' mass, a_{radial} is the radial acceleration, μ is the static friction coefficient, and θ is the wedge angle introduced in Sec. 2.1, defined by $\theta = \arcsin(y/R)$, y and R being the distance from the contact point to the lens' axis and the radius of curvature of the lens' surface. Equation (9) represents the friction force exerted by the spring plates, which will act against any external force applied on the system. At the same time, the stresses on the lenses induced by those forces must be lower than the fracture limit given in Sec. 2.3. The two parameters that can be tuned to achieve the required radial force are the normal force that is applied to the lens and the distance from the optical axis to the contact point. From Eq. (9), given the friction coefficient of the glass and the metal, $\mu = 0.15$[19] and, taking into account the force decomposition, the maximum normal forces that are applied by the springs are 117 N for the CaF_2 lens and 103 N for the S-FTM16 lens. With these values and the Yoder formulation for tangential and tororidal contacts, the applied stresses on the lenses is ~1 MPa. Comparing this with the maximum stress values calculated in Sec. 2.3, we see that the lenses are held safely for transportation. Table 1 shows the physical properties of the lenses of the collimator of FRIDA that are necessary to calculate the corresponding normal forces.

3.2 *Outer Cell*

To reduce the temperature differences between the lenses and their mechanical mount, the optomechanical cell is supported with a heat flux manifold, as shown in Fig. 1(a). This has been optimized using a finite element analysis model.

Table 1 Physical properties of the lenses, showing the two radii of curvature, R_1 and R_2, diameter (D), clear aperture (A), mass (W), contact point distance from axis (y), and wedge angle (θ).

Lens	Material	R_1 (mm)	R_2 (mm)	D (mm)	A (mm)	W (kg)	y (mm)	θ (deg)
Divergent	S-FTM16	225.2	117.5	92	73	0.215	41.25	10.0
Convergent	CaF_2	122.0	−298.2	92	73	0.228	41.25	27.7

4 Experimental Tests

The tests for validating the optomechanical mount presented in Sec. 3 have been designed to verify the requirements exposed in Sec. 2, in particular, to determine the autocentering capability of the lenses when exposed to accelerations of 10 g or larger (Sec. 5) and when achieving the thermal equilibrium at operation conditions at 150 K (Sec. 6). The autocentering mount should ensure the preservation of the final image quality of the instrument.

For the tests, we used the optomechanical mount of the collimator with two test lenses of glass Schott BK7, with the same geometrical dimensions as the CaF_2 and S-FTM16 doublet. The thermal conductivity of CaF_2 is significantly higher than that of BK7 (9.71 $W/m \cdot K$ for the former and 1.114 $W/m \cdot K$ for the later); hence, the CaF_2 lens will be able to adjust to changes in temperature more quickly than the BK7 lens. As for the S-FTM16 lens, its thermal conductivity is slightly lower than that of BK7 (0.947 $W/m \cdot K$ for S-FTM16); however, the temperature differences obtained for the divergent lens leave enough margin to compensate for this little difference with confidence.

5 Impact Tests

5.1 *Experimental Setup for Impact Tests*

Impact tests refer to the lenses undergoing similar accelerations to those that they will suffer during transportation to the telescope's site. The frictional forces exerted by the optomechanical support are such that the lenses will not move when exposed to accelerations up to 10 g. With this test, we demonstrate that, even with larger acceleration in play, the lenses move, but the autocentering mount allows them to perfectly return to their nominal position. These tests are done with the lenses assembled in their optomechanical mount on a test table, at room temperature and atmospheric pressure. The optomechanical system underwent accelerations greater than 10 g by being hit with a mass hanging from a pendulum at different heights. The experimental setup for the tests is shown in Fig. 2. Further details may be found in Sánchez et al.[14]

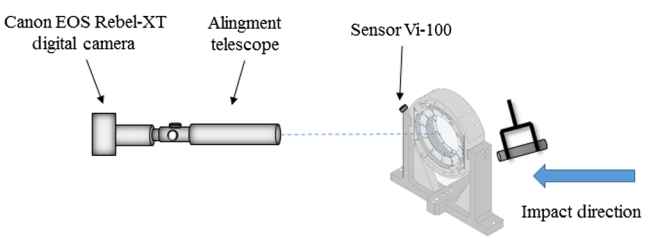

Fig. 2 Experimental setup for impact tests.

The applied acceleration was measured with a vibrometer (Vi-100) placed on the opposite side of the impact point. Using an oscilloscope connected to the vibrometer, we obtained a complete record from the time of impact until the end of the vibration. The vibration frequency of the test table is about three-orders of magnitude lower than that of the collimator system (Hz versus kHz), showing that it is the collimator system that actually moves after the hit. This was confirmed by measuring the acceleration of the test table with the vibrometer fixed to the table. The methodology and experimental layout to measure the movement of the system was as follows:

- A flat surface was polished on a section around the vertex of the spherical front face of the convergent lens and coated with an aluminum layer.
- A flat mirror with a central hole was mounted in front of the convergent lens.
- Using an alignment telescope working in autocollimation (Bronson-K&E 2022) with a reticle and a light source, we sent the light from the reticle to the two-mirror system described above. The image of the two reflected reticles was registered using a computer-controlled digital camera (Canon EOS Rebel-XT). When the test acceleration was applied, the outer mirror moved longitudinally, but the lens moved rotationally around the center of curvature of one of its surfaces and tilted accordingly. With the digital camera, we measured the relative displacement of the two reflected reticles due to a tilt in the convergent lens.
- The impact was repeated and recorded in a total of eight events. The position of the lenses during the post-impact vibrations was measured with a series of three pictures: one before the impact, a second one immediately after the impact, and a third one 5 mins later. We have no means to measure the exact time at which the second picture is taken; this one is only to verify that the system is in fact moving, but it will only show a qualitative estimation. Images were then analyzed with software that finds the centers of the reticles by means of Gaussian fits to the perpendicular cross sections at each point of each reticle, with uncertainties of less than one projected pixel in the final positions. Results from the eight events were averaged, and the measurement errors were estimated as the standard deviation of the results in the eight events.

5.2 *Results of Impact Tests*

With the experimental setup and methodology described in Sec. 5.1, we measured the position of the lenses of the collimator when exposed to accelerations lower and greater than

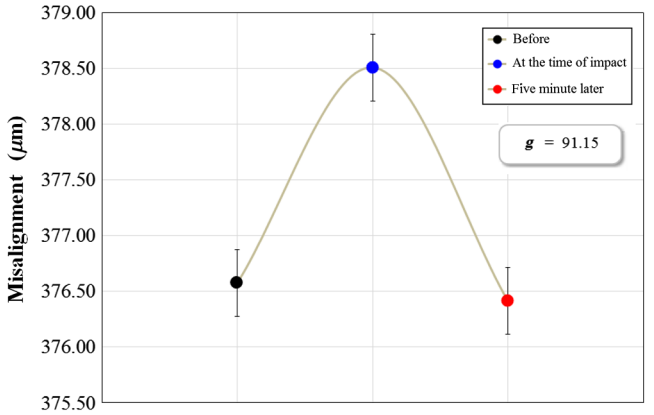

Fig. 3 Relative position of the lenses at the three times: before the impact, immediately after the impact, and 5 min later.

10 g. The acceleration of the collimator, normalized to the acceleration of gravity, is given as

$$a = \frac{1}{g}\frac{m}{Mt}\sqrt{2hg}, \tag{10}$$

where $m = 0.268$ kg is the mass of the body that hits the collimator, $M = 2.970$ kg is the total mass of the collimator (including lenses and mechanics), h is the initial height of the hitting body, and t is the response time of the system. The latter was measured by connecting the vibrometer to an oscilloscope and measuring the time from the moment of impact until the first maximum or minimum.

When accelerations lower than 10 g were applied, we could not record a displacement of the lenses beyond the measurement errors of ± 0.3 μm. For the strongest event, with $h = 0.008$ m and $t = 0.00004$ s (as measured with the oscilloscope), we get that the maximum acceleration with which we hit the collimator was 91.15 g.

The relative position of the lenses for this event (with respect to the initial position) is shown in Fig. 3 at three times: right before the impact, immediately after the impact, and 5 min later. The lenses move at least 2 μm after the impact, and the vibration is then quickly damped.

We have demonstrated that the lens' support is such that the lenses do not move when exposed to accelerations of 10 g or lower. Furthermore, even when the accelerations that they suffer are much greater than this value, lenses do not move beyond requirements, and, furthermore, they return to their original position, hence showing the autocentering capability of the optomechanical system after vibrations.

6 Cryogenic Tests

6.1 *Experimental Setup for Cryogenic Tests*

For the cool-down and warm-up tests, the optomechanical mount was verified in the FRIDA cold test facility (FCTF), a cryostat and cold optical bench developed and built at the IA-UNAM specifically for the FRIDA subsystems tests. In these tests, we measured individual movements of the two lenses inside the optomechanical mount from an external mechanical reference. This is not a simple process since once the cryostat has been closed, there is no direct access to the collimator system until the test is finished. The methodology and experimental layout were as follows.

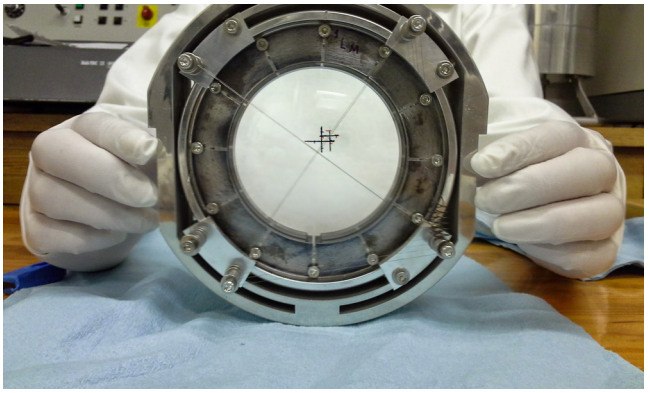

Fig. 4 Reticles drawn on the inner surfaces of the two lenses.

- A cross-shaped reticle was drawn on the inner surface of each lens in the doublet (i.e., on the two encountering surfaces of the doublet), as shown in Fig. 4.
- The centering of the two lenses within the mechanical cell was done *a priori* with ALBatros, an alignment bench designed and built at the IA-UNAM for this specific purpose. ALBatros allows optical systems to be mounted with the optical axis and the mechanical axis aligned with a precision of ± 14 μm and evaluation of the optical axis decenter resultant from the combination of lenses within a common cell with a precision of about ± 2 μm.
- As a physical reference to measure the movements of the lenses within their cell, we placed two crossing wire reticles held to the mechanical mount of the doublet cell at the heat flux manifold such that the crossings of the two reticles lie at the mechanical axis of the optomechanical mount.
- To register the temperature of the lenses and evaluate temperature differences, we placed two temperature sensors on each lens, one near the edge and another near the center (Fig. 5). Nine other sensors were placed at different points of the mechanical system.
- The optomechanical system was placed on the cold bench of FCTF. The cryostat has two opposite windows at the appropriate height; one is illuminated with a light source and images are registered from the other one. Images were recorded using the alignment telescope and digital camera system from Sec. 4. The experimental setup for the test is shown in Fig. 6.

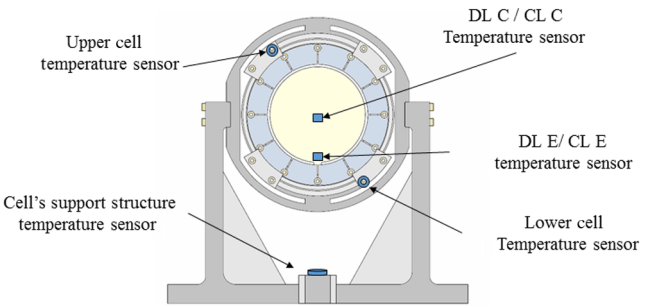

Fig. 5 Test collimator system mounted on FCTF's cold bench and location of temperature sensors.

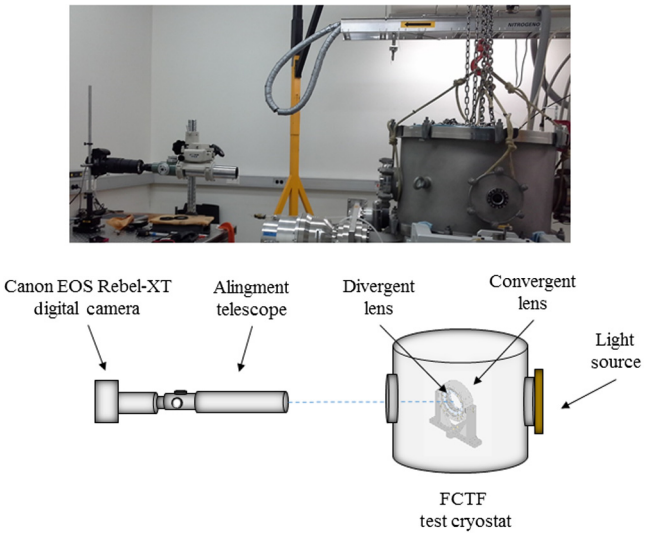

Fig. 6 Experimental setup for cryogenic tests.

- Images were analyzed with software that finds the centers of the wire and draws reticles by means of Gaussian fits to the perpendicular cross sections at each point of each reticle, with uncertainties of less than one projected pixel.

In principle, for the procedure described above to be valid, it is necessary that the optical axis of the measurement system (alignment telescope plus digital camera) is perfectly well aligned with the mechanical axis of the collimator. This is not trivial because of the inner movements of the cold structure of the cryostat when cooled down (i.e., the cold structure translates and rotates when cooled, hence losing the alignment), but it is absolutely crucial since we demonstrated that small misalignments of the measurement system with respect to the collimator axis, though not noticeable to the naked eye, produce significant variations in the movements of the reticles registered with the digital camera, hence giving rise to potentially fake results. Therefore, to avoid these misalignment problems, we took the following strategy.

The alignment telescope plus digital camera was deliberately slightly misaligned with respect to the collimator mechanical axis in such a way that the two wire reticles appeared clearly away from each other at the digital camera image, so a measurement of the separation between the two was possible. In this manner, the optical axis of the measurement system, z', is clearly inclined with respect to the collimator mechanical axis, z. The inclination angle between the two axes is given by the distance between the crossings of the two wire reticles, measured by the digital camera (on the $x'y'$ plane), divided by the distance between the crossings of the two wire reticles along the z axis. Once we know the inclination angle, the distance from the wire reticles and the lenses, and the distance between the two lenses within the optomechanical mount (along the z axis), we can write a coordinate transformation from those measured with the digital camera, in the inclined reference system, S' (on the $x'y'$ plane), to those in the designed reference system, S (on the xy plane). By means of a few simple geometrical calculations, it can be shown that the coordinates on the xy plane may be expressed as a function of the coordinates measured on the $x'y'$ plane as

$$x = x' \pm \alpha(D + e), \tag{11}$$

$$x = x' \pm \alpha(D + e + d), \tag{12}$$

respectively, for the divergent lens (directly in front of the measurement system) and the convergent lens (behind the divergent lens), where α is the inclination angle between z and z', D is the distance from the closest wire reticle to the lenses to the first surface of the divergent lens, e is the on-axis thickness of the divergent lens, and d is the on-axis distance from the divergent and convergent lenses. Similar expressions can be found for the y coordinate.

6.2 *Results of Cryogenic Tests*

The cryogenic performance of the optomechanical system was verified through two identical tests including two thermal cycles each (four in total), following the experimental setup and methodology described in Sec. 6.1. For simplicity, we only present one of these tests, which includes two continuous cycles of cooling down to the operational temperature and warming up to the ambient temperature (i.e., without taking the collimator system out of the cryostat in between cycles), using a closed cycle cryogenic cooler for cool-downs and heating resistances for warm-ups (this will be the usual warm up procedure at the telescope). The second test showed equivalent results.

Before the start of the cryogenic run, the system was prealigned in the optical bench ALBatros. The resultant relative misalignment of the two lenses after this process was 14 μm.

The temperature of the system and the movement of the two lenses were registered during the entire two cycles, allowing for the stabilization of the system at operation temperature and room temperature before starting the second cycle.

Figures 7(a) and 7(b) show the temperature readings registered at the 13 sensors located at the lenses, mount, and cryostat during the two cycles. Temperature sensors CL E and CL C correspond to the edge and center of the convergent lens (which corresponds to the CaF_2 lens), and DL E and DL C correspond to the edge and center of the divergent lens (which corresponds to the S-FTM16 lens). Each cycle extends through an approximate time of 400 h. In both cycles, lenses achieve the operational temperature after about 70 h and stabilize after about 100 h. In detail, the first cool-down started at 0 h, the first warm-up at 290 h, the second cool-down at 400 h and the second warm-up at 600 h.

Figure 8 shows the movement of the divergent and convergent lenses within their optomechanical mount. The origin of the coordinate system was defined as the position of the two lenses at the beginning of the experiment, prealigned and at the ambient temperature. During the cooling process, the two lenses move uniformly until operation temperature is reached and then return back to their original position within an error of about ± 10 μm. The second cycle starts at that last position of the first cycle, with a similar movement as before. The relative misalignment of one lens with respect to the other during the two complete cycles is shown in Figs. 7(c) and 7(d). Here we see that, despite the joint movement of

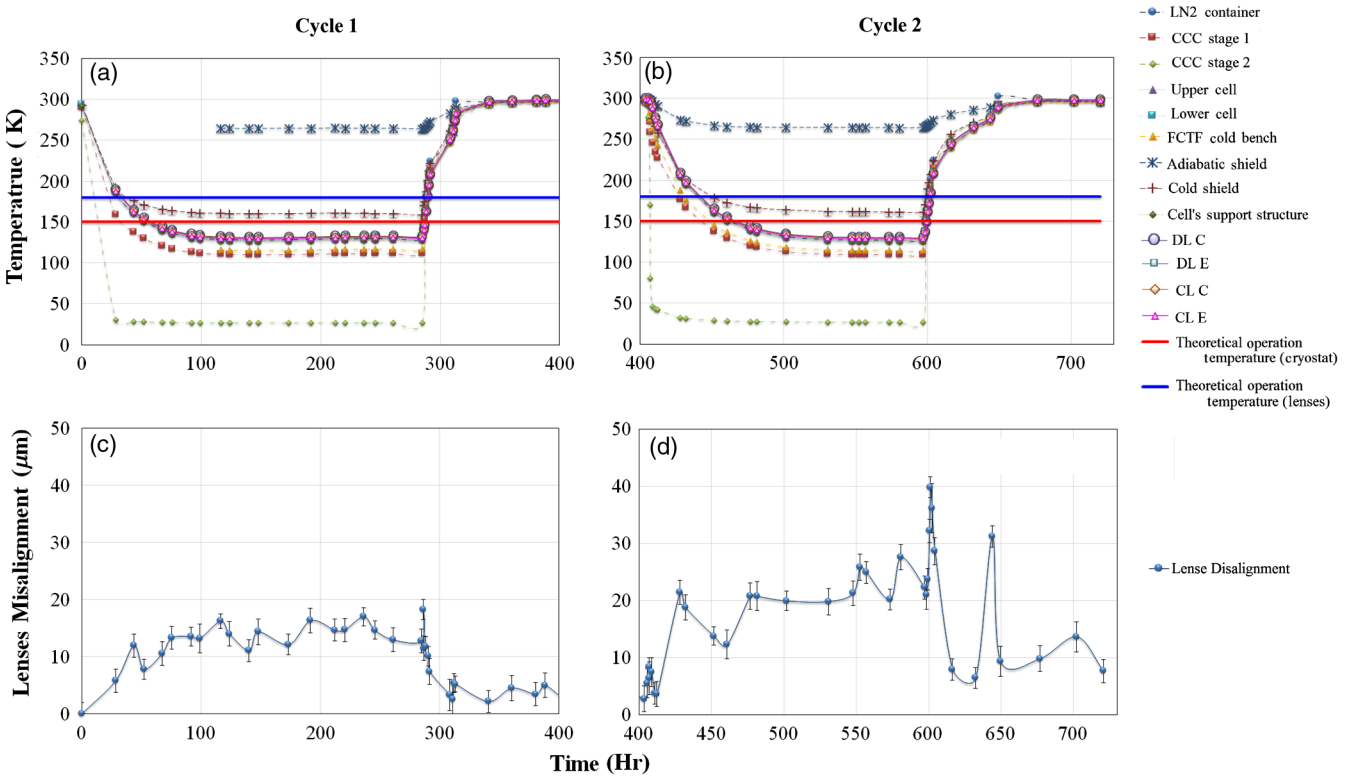

Fig. 7 Thermal behavior of the test collimator system inside FCTF during (a and b) the two cycles and (c and d) relative misalignment of the two lenses.

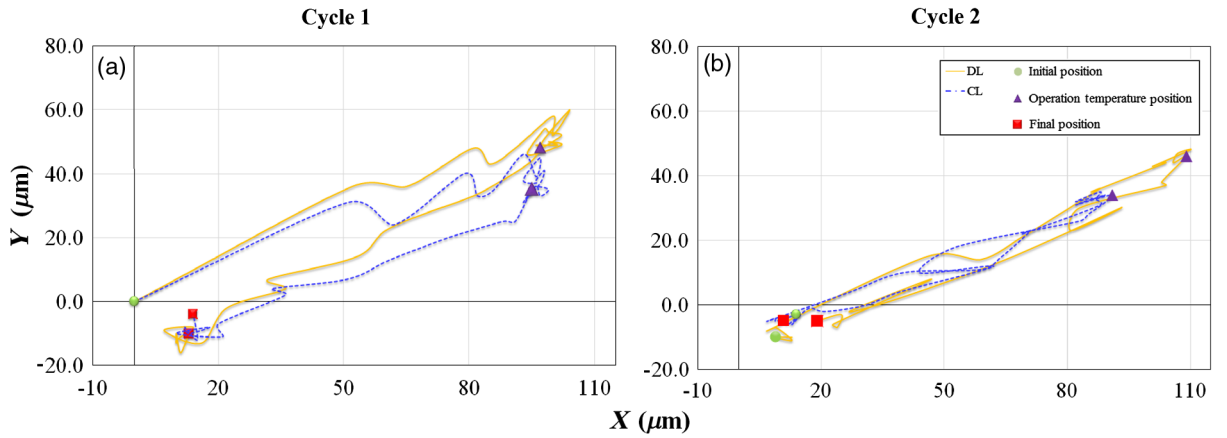

Fig. 8 Movement of the divergent and convergent lenses with respect to the optomechanical mount.

the two lenses, the maximum misalignment of one with respect to the other is only about 20 μm. In combination with the misalignment measured at the beginning of the tests, prior to the cryogenic runs, in the worst case, these sum to a maximum relative misalignment of about 34 μm. The relative misalignment is slightly larger when the warming up begins, although this is not relevant since we see that lenses return to their original position when the ambient temperature is reached. The discontinuities observed around hours 310 and 640 may be explained because the heating resistances needed to be switched off at night and switched on again in the morning. In any case, the observed misalignment is well below the maximum allowed values given by the Zemax tolerancing analysis.

The error bars in Figs. 7(c) and 7(d) have been propagated from the measurement error, which was estimated as the standard deviation of a sample of 10 images for each case.

Temperature differences between the center and the edge of each lens during the thermal cycles were evaluated with the data from Figs. 7(a) and 7(b). These are shown in Fig. 9. We see that temperature differences are always less than 1 K for the convergent lens (corresponding to the CaF_2 lens) and less than 1.2 K for the divergent lens (corresponding to the S-FTM16 lens). These values are well below the threshold values defined in Sec. 2.4 (5.5 and 58.3 K, respectively). Therefore, the fracture probability is extremely low even during cool-downs and warm-ups due to the heat flux manifold,

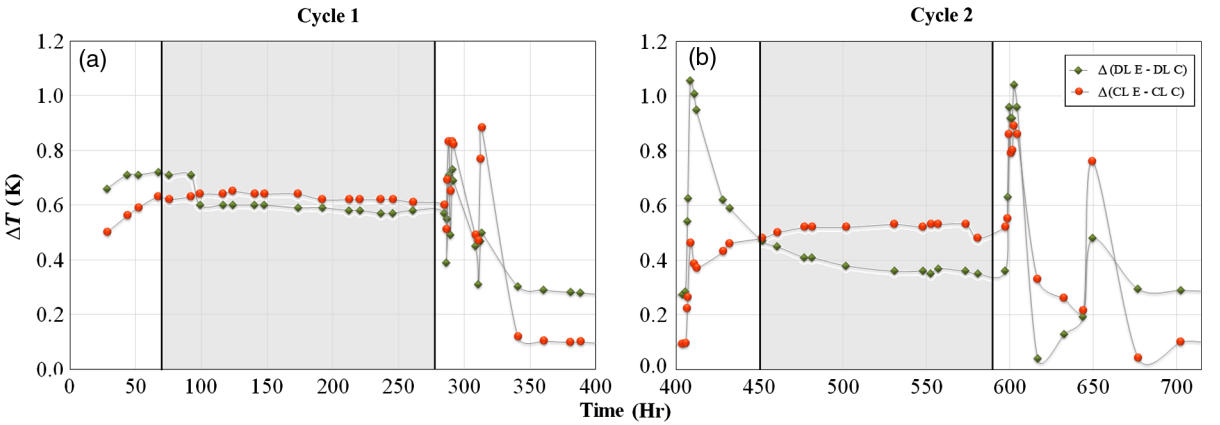

Fig. 9 Temperature differences between the center and the edge of the divergent and convergent lenses during the two thermal cycles. The shaded regions represent the intervals of operation temperatures.

which allows for a passive uniform heat flux between the mount and the lenses.

Focusing now our attention at the intervals where the operational temperature has been reached (70 to 290 h in the first cycle and 450 to 600 h in the second), in Fig. 9, we observe that temperature differences between the center and the edge of each lens is less than 0.7 K. Comparing this value with that of Sec. 2.5 (1.27 and 5.96 K, respectively), we see that these are sufficient to not induce significative changes in the refractive index of the materials that degrade image quality beyond requirements.

Finally, after the cryogenic runs were finished, and the collimator system was taken out of the cryostat, we measured again the relative misalignment in the optical bench ALBatros, giving a value of 14 μm, exactly the same as before the experiment, confirming the validity of the results from above, and the excellent performance of the optomechanical mount.

7 Summary and Conclusions

The optomechanical system presented in this work has been designed to support the lenses from a cryogenic achromatic lens doublet as part of the diffraction limited instrument FRIDA.[12,13] This system has the following characteristics:

1. By design, the lenses move in a rotational manner inside the optomechanical cells, around the center of curvature of the surface in contact with the fixed mechanical support.
2. Once aligned, the support system maintains the alignment within requirements under accelerations greater than 10 g and during thermal cycles, by orders of magnitude better than the corresponding autocentering potentials.
3. The temperature differences between the center and the edge of each lens never exceed the fracture value for the equivalent CaF_2 and S-FTM16 lenses during cool-downs and warm-ups, and neither exceed the values that will induce significative changes in the refractive index of the materials that degrade image quality beyond requirements during operation.

We have demonstrated an excellent performance of the proposed optomechanical mount for the lenses of the collimator of FRIDA, achieving much better results than the corresponding autocentering potentials provided that we are able to prealign the lenses to within ± 14 μm precision. Regarding the other lens systems of FRIDA, with better autocentering potentials, we presume that this mount will work similarly well, though this ought to be tested in the future. In general, we postulate that the optomechanical mounting method presented in this article will give an excellent performance for cryogenic mounts of this kind, with similarly high image quality requirements.

Acknowledgments

The authors are grateful to our home institution for their support and CIDESI (Centro de Ingeniería y Desarrollo Industrial), Querétaro, for their collaboration on the mechanical design and manufacturing, with special thanks to Dr. Alan M. Watson and Dr. José Alberto López for many useful comments. This work has been funded by Encuentros Astrofísicos Blas Cabrera, Grupo Santander (UNAM—IAC); Programa de Apoyo a Proyectos de Investigación e Innovación Teconológica (PAPIIT) (IT116311, IT100913); and Consejo Nacional de Ciencia y Tecnología (CONACYT) (2009-01-122664).

References

1. P. R. Yoder, Jr., *Opto-Mechanical Systems Design*, 4th ed., Marcel Dekker, New York (2006).
2. E. Fischer, B. Tadic-Galeb, and P. Yoder, *Optical System Design*, 2nd ed., McGraw Hill, New York (2008).
3. A. Ahmad, *Handbook of Optomechanical Engineering*, 2nd ed., CCR Press, Boca Raton (1997).
4. B. A. McLeod et al., "MMT and Magellan infrared spectrograph," *Proc. SPIE* **5492**, 1306 (2004).
5. T. P. O'Brien and B. Atwood, "Lens mounting system for cryogenic applications," *Proc. SPIE* **4841**, 398–402 (2003).
6. H. Baumeister et al., "Cryogenic engineering for omega 2000: design and performance," *Proc. SPIE* **4841**, 343–354 (2003).
7. R. L. Edeson et al., "The mechanical and thermal design and analysis of the VISTA infrared camera," *Proc. SPIE* **5497**, 508–519 (2004).
8. T. Kvamme et al., "Mounting of large lithium fluoride space-based optics," *Proc. SPIE* **5877**, 58770T (2005).
9. T. R. Froud et al., "Cryogenic mounts for large fused silica lenses," *Proc. SPIE* **6273**, 62732I (2006).
10. L. J. Lizon and G. Huster, "Mounting of large lenses in infrared instruments," *Proc. SPIE* **6273**, 62733M (2006).
11. W. Zschommler, "Precision optical glassworking: a manual for craftsmen and designers,"Macmillan and SPIE, London and Bellingham, Washington (1984).

12. S. Cuevas et al., "FRIDA: the infrared imager and integral field spectrograph for the adaptive optics system of GTC," *New Astron. Rev.* **50**(4–5), 389–391 (2006).
13. J. A. López et al., "FRIDA: integral-field spectrograph and imager for the adaptive optics system of the Gran Telescopio Canarias," *Proc. SPIE* **6269**, 62693R (2006).
14. B. Sánchez et al., "FRIDA diffraction limited NIR instrument, the challenges of its verification processes," *Proc. SPIE* **9150**, 91501R (2014).
15. D. B. Leviton et al., "Temperature-dependent refractive index measurements of CaF_2, Suprasil 3001, and S-FTM16 for the Euclid near-infrared spectrometer and photometer," *Proc. SPIE* **9578**, 95780M (2015).
16. C. A. Klein, "Flexural strength of optical infrared-transmitting windows materials: bimodal Weibull statistical analysis," *Opt. Eng.* **50**(2), 023402 (2011).
17. "TIE-33: design strength of optical glass and Zerodur," 2015, Advanced optics, Schott, http://www.schott.com/d/advanced_optics/b0df0a6f-e89b-4483-88fb-bdb2f7ba8792/1.0/schott_tie-33_bending_strength_of_optical_glass_and_zerodur_eng.pdf?highlighted_text=TIE-33 (06 December 2016).
18. "TIE-32: thermal loads on optical glass," Advanced optics, Schott, 2004, http://www.schott.com/d/advanced_optics/768b0d65-8838-4021-b7a9-5c06647d055c/1.1/schott_tie-32_thermal_loads_on_optical_glassus.pdf (06 December 2016).
19. J. C. Burton, P. Taborek, and J. E. Rutledg, "Temperature dependence of friction under cryogenic conditions in vacuum," *Tribol. Lett.* **23**(2), 131–137 (2006).

Beatriz Sánchez obtained her BSc degree in physics and her master's degree in electronics engineering from the Universidad Nacional Autónoma de México (UNAM). She has been involved for more than 25 years in astronomical instrumentation projects at the Instituto de Astronomía, UNAM, the last decade as a project manager for Gran Telescopio Canarias instruments.

Biographies for the authors are not available.